Cellular Model for Induction of Drip Loss in Meat

Ian Henry Lambert,*,† Jacob Holm Nielsen,‡ Henrik Jørgen Andersen,‡ and Niels Ørtenblad‡

Biochemical Department, The August Krogh Institute, Universitetsparken 13, DK-2100 Copenhagen, Denmark, and Danish Institute of Agricultural Sciences, Research Centre Foulum, P.O. Box 50, DK-8830 Tjele, Denmark

Drip loss from porcine muscle (M. longissimus dorsi) contained high concentrations of K^+ (∼135 mM) and organic osmolytes, for example, taurine (∼15 mM), as well as significant amounts of protein (∼125 mg·mL^{-1}). Thus, the drip reflects release of intramuscular components. To simulate events taking place at the time of slaughter and leading to release of osmolytes and subsequent formation of drip loss, C2C12 myotubes were exposed to anoxia and reduction in pH (from 7.4 to 6.0). Anoxia and acidification increased the cellular Ca^{2+} concentration ($[Ca^{2+}]_i$) at a rate of 22−32 nM·min^{-1}. The anoxia-induced increase in $[Ca^{2+}]_i$ was mainly due to influx via sarcolemmal Na^+ channels. As mammalian cells swell and release lysophospholipids during anoxia, C2C12 cells and primary porcine muscle cells were exposed to either hypotonic shock or lysophosphatidylcholine (LPC) and the release of taurine was followed. The swelling-induced taurine efflux was blocked in the presence of the anion channel blocker (DIDS), the 5-lipooxygenase inhibitors (ETH 615-139 and NDGA) but unaffected by the presence of vitamin E. In contrast, the LPC-induced taurine release was unaffected by DIDS but abolished by antioxidants (butylated hydroxytoluene and vitamin E). Thus, stress-induced taurine release from muscles may precede by two different mechanisms, one being 5-lipooxygenase dependent and the other involving generation of reactive oxygen species. A model for the cellular events, preceding formation of drip in meat, is presented.

Keywords: *C2C12 cells; primary porcine muscle cells; organic osmolytes; taurine; calcium; anoxia; LPC; volume regulation*

INTRODUCTION

The main constituent of meat is water, compromising ∼75% of its weight (*1, 2*). About 90% of the water is bound in the muscle cell, and the rest is present in the interstitium. As 80% of the volume of the muscle is occupied by myofibrils, it is generally accepted that 90−95% of the water in the muscle cell is present between the myofibrils and 5% is chemically bound to the charged groups of the intracellular muscle proteins (*3*).

The water-holding capacity (WHC), that is, the ability of meat to retain water, affects the extent of water exudation from the surface of the meat and thereby the amount of expelled water in the finished retail packs. This affects the appearance of the meat and thereby the consumers' perception of its quality. Moreover, the WHC of meat may influence the sensory quality, as a high cooking loss implies that the meat is sensed as being less juicy and more tough (*4*). As loss in quality and weight imply financial loss, the meat industry has a huge interest in optimizing the WHC, that is, limiting loss of fluids (drip loss) during slaughter and subsequent manipulations (*5*).

Water loss, mainly evaporation from carcasses, during 2 days in chill, is estimated at 0.1−1.0% of the initial weight (*6*). However, when the meat is cut, the muscle surface is increased and the drip loss during 4 days under chilling conditions increases to 2−6% of the lean meat (*7*). The biochemical, physiological, and structural events that are initiated by slaughtering and which lead to drip loss are complex and poorly understood. However, loss of osmolytes and cell water, following osmotic perturbation, hormonal stimulation, and limitation in oxygen supply (anoxia), has been described in a variety of mammalian cells. This knowledge provides an obvious starting point in the understanding of the initial processes leading to water reorganization in muscle during its conversion to meat. Mammalian cells, exposed to a hypotonic solution, swell initially as more or less perfect osmometers; thereafter they regulate their cell volume back toward the original value (see refs *8* and *9*). The initial cell swelling reflects the high water permeability of the cells, whereas the subsequent reduction in cell volume reflects net loss of osmotically active cytoplasmic solutes (KCl, polyols, methylamines, and amino acids) and cell water (see refs *8* and *9*). Taurine, 2-aminoethanesulfonic acid, is an important organic osmolyte in many types of mammalian cells, and loss of taurine is often taken to indicate a reduction in cell volume. The functional properties of the transport pathways for inorganic/organic osmolytes, as well as the mechanisms by which they are activated by the cell swelling, are only partly understood. For some cell lines it has been demonstrated that swelling-induced activation of taurine release involves phospholipase A_2 (PLA_2) and 5-lipoxygenase (5-LO) activities (see refs *10* and *11*). Ca^{2+} and calmodulin seem to play a key role in the regulation of the activity of the phospholipase and proteases, whereas reactive oxygen species (ROS) interfere with the 5-LO activity, that is, leukotriene

* Author to whom correspondence should be addressed (telephone +45 3532 1697; fax +45 3532 1567; e-mail ihlambert@aki.ku.dk).

† The August Krogh Institute.

‡ Danish Institute of Agricultural Sciences.

10.1021/jf010121y CCC: $20.00
Published on Web 09/27/2001

formation (see ref *12*). Release of KCl from mammalian cells is also initiated by an increase in the cellular free Ca^{2+} concentration ($[Ca^{2+}]_i$) (see ref *9*). More recently, it has been shown that taurine is released also under isotonic conditions following addition of lysophosphatidylcholine (LPC) (*13*, *14*). Lysophospholipids, produced by, for example, PLA_2-mediated hydrolysis of membrane phospholipids, are natural component of the serum. However, accumulation of free LPC has been reported in ischemic myocardium (*15*) and in oxidized lipoproteins (*16*). The physiological effect of LPC is concentration dependent; that is, specific controlled effects (generation of superoxides, Ca^{2+} mobilization, and release of arachidonic acid and nucleotides) seem to dominate at low LPC concentrations (<15 μM), whereas a general membrane permeabilization (release of creatine kinase) occurs at high LPC concentrations (>20 μM). In the case of HeLa cells it appears that taurine release, elicited by the addition of 5−10 μM LPC, occurs in a process that involves ROS production, which is modulated by a calmodulin/calmodulin-dependent kinase (CaMKII) as well as tyrosine kinase (*13*, *14*).

Anoxia/ischemia, which represents the situation in muscle cells upon slaughter, is known from other cell systems to be associated with (i) increases in $[Ca^{2+}]_i$ and the cellular Na^+ concentration, (ii) activation of Ca^{2+}-dependent and Ca^{2+}-independent forms of PLA_2, (iii) increases in cell volume, (iv) cellular acidification, and (v) reduction in the cellular content of ATP and creatine phosphate (PCr) (see ref *17*). During stress situations associated with transportation and stalling of livestock, the stunning procedure, and handling of carcasses, the muscles are inevitably exposed to massive hormonal stimulation, anoxia, and metabolic stress. Taken together, we have a scenario that affects the muscular content of osmolytes and cell water and which could lead to the formation of drip loss.

The aim of the present study was to set up a model for initial events in the formation of drip loss. We have emphasized on (i) the qualitative characterization of drip loss and (ii) the effect of anoxia, acidification, osmotic perturbation, and exposure to lysophospholipids on regulation of $[Ca^{2+}]_i$ and the cellular content of organic osmolytes. We have used the mouse myoblastic cell line C2C12 and primary porcine muscle cells and characterized systems responsible for anoxia-induced increase in $[Ca^{2+}]_i$ as well as signal pathways involved in the release of organic osmolytes.

MATERIALS AND METHODS

Chemicals. Antibiotics, foetal bovine serum (FCS, no. 10106-169), trypsin, and Dulbecco's modified Eagle's medium (high glucose) with L-glutamine (DMEM, no. 42430025) were from Life Technologies (Naperville, IL). [^{14}C]Taurine was from NEN Life Science Products, Inc. (Boston, MA). Fura-2/AM, Pluoronic F-127 and ionomycin were purchased from Molecular Probes (Eugene, OR). Saxitoxin was obtained from Calbiochem (Bad Soden/TS, Germany). ETH 615-139 was donated by Dr. I. Ahnfelt-Rønne (Løvens Kemiske Fabrik, Denmark). Collagenase was from Medinova (Hellerup, Denmark). Matrigel was from Becton Dickinson. All other compounds were from Sigma Chemical Co. (St. Louis, MO).

Inorganic Media. Phosphate-buffered saline (PBS) contained 137 mM NaCl, 2.6 mM KCl, 6.5 mM Na_2HPO_4, and 1.5 mM KH_2PO_4. Isosmotic KCl solution contained 150 mM KCl, 1.3 mM $CaCl_2$, 0.5 mM $MgCl_2$, and 10 mM HEPES. Hyposmotic KCl solution was obtained by reduction of the KCl in the isosmotic KCl solution to 95 mM, with the other components remaining unchanged. Krebs−Hepes buffer (KHB) contained 118.0 mM NaCl, 4.7 mM KCl, 1.2 mM KH_2PO_4, 4.2 mM $NaHCO_3$, 1.3 mM $CaCl_2$, 1.2 mM $MgSO_4$, 10.0 mM HEPES, and 10 mM d-glucose. pH was in all solutions adjusted at 7.40.

Muscle Cell Cultures. The taurine flux and Ca^{2+} measurements were performed using a myoblast cell line (C2C12) originally derived from the thigh muscle of the mouse (*18*; American Type Culture Collection, Manassas, VA). A clone of the cell line, which fused and formed myotubes, was isolated and used in the experiments. The clone was raised in a 75 cm^2 culture flask in 10 mL of medium consisting of DMEM with 10% (v/v) FCS. The medium was supplemented with 100 IU/mL penicillin, 100 μg/mL streptomycin sulfate, 3 μg/mL amphotericin B, and 20 μg/mL gentamycin. Cells were maintained in an atmosphere of 95% air and 5% CO_2 at 37 °C. At confluence, cells were split and seeded for either intracellular Ca^{2+} level assays or taurine flux measurements. For the intracellular Ca^{2+} measurements, cells were cultured on laminin-coated glass coverslips (10 × 43 mm) in four-well multidishes (Nunc 366148) with two coverslips in each well. The initial plating density was 6000 cells/cm^2, and cells were grown to confluence on medium with 10% FCS. At confluence, the coverslips were removed to new four-well multidishes with medium and 4% FCS. Within 2−3 days cells fused to nonproliferative, multinucleated myotubes and were used for estimation of intracellular Ca^{2+} measurements. For the taurine efflux measurements, cells were seeded in six-well Primaria multiwell plates (35-mm diameter, Becton Dickinson Labware) at a density of 2000 cells/cm^2 and grown in media with 10% FCS until near confluence; thereafter, the FCS was reduced to 4% and the cells left to fuse into myotubes. Primary cells were isolated from M. semimembranosus from Danish landrace pigs using modifications of Bischoff's original method (*19*). The muscle tissue was excised, finely chopped, and digested three times for 20 min in 20 mL of PBS containing 1% glucose, 1.5 mg/mL collagenase II, 0.25% trypsin, and 0.01% DNase. Following digestion the cells were transferred to a primary growth medium (PGM; DMEM with 10% FCS and 10% horse serum), triturated, centrifuged (1000 rpm, 10 min, 4 °C), resuspended, and filtered through a 200 μm and subsequently a 50 μm Nytex filter. Filtered cell suspension was placed on a 20% Percoll layer and spun for 5 min at 20000*g*. The resultant cell layer was retrieved and seeded at a density of 2000 cells/cm^2 in Nunc six-well plates (35-mm diameter) coated with Matrigel and grown in PGM until near confluence. Nearly confluent cells were left to fuse into myotubes in DMEM with 2% FCS and 1 μM insulin.

Determination of Free Cytoplasmic Ca^{2+} Concentration. The C2C12 cells grown on coverslips were washed in KHB. The cells were incubated in KHB containing 3 μM fura-2/AM and 0.04% Pluoronic F-127 for 1 h at 25 °C, washed three times with KHB, and incubated for 15 min at room temperature to allow de-esterification of the fura-2/AM. The coverslips were mounted in a custom-made holder, placed vertically in a 10-mm path length cuvette, and analysis was performed on a Perkin-Elmer LS50B luminescence spectrometer. The emission wavelength was 510 nm, and the subsequent ratio after excitation at 340 nm and 380 nm (the 340 nm/380 nm ratio, R) were collected every 2 s. The background signal (cells without fura-2) was subtracted from the fluorescence data before the ratio values were converted to free Ca^{2+} concentrations according to the equation $[Ca^{2+}] = K_d(R - R_{min})/(R_{max} - R)(S_{f,2}/S_{b,2})$ (*20*). For each series of eight experiments the ratio signal was calibrated by adding 5 μM ionomycin (R_{max}) and 8 mM EGTA (R_{min}), respectively, and a K_d of 224 nM was experimentally determined using a standard Ca^{2+} calibration buffer kit (Molecular Probes). The linear increase in free cytoplasmic Ca^{2+} concentration $[Ca^{2+}]_i$ (nM·min^{-1}) was determined in the time range of 2−20 min following onset of the experiment (see Figure 1A).

Efflux Measurements−Estimation of Rate Constants. Taurine efflux from C2C12 and primary porcine muscle cells was measured at room temperature (~20 °C) as described previously (*13*, *21*). Briefly, cells plated in polystyrene dishes and adapted to 4% FCS serum were loaded with [^{14}C]taurine

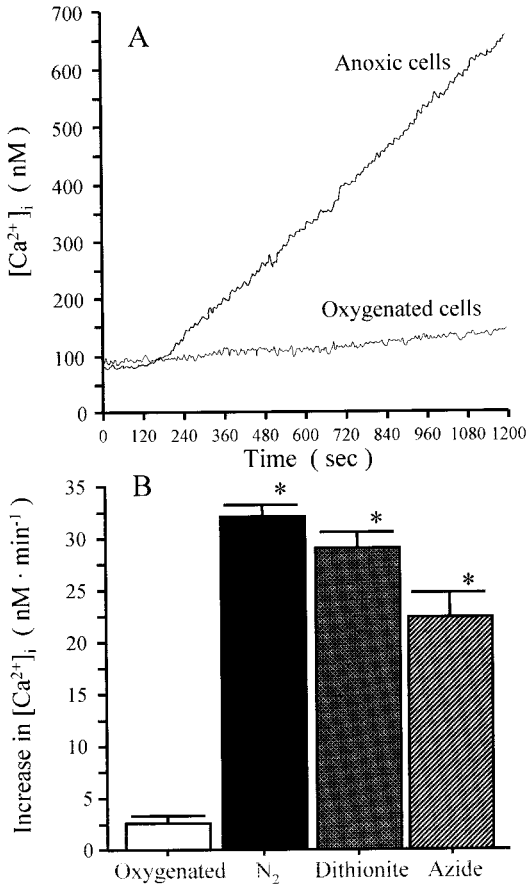

Figure 1. Effect of anoxia on $[Ca^{2+}]_i$: (A) Time course for $[Ca^{2+}]_i$ in oxygenated cells and anoxic (N_2 treated) cells; (B) increase in $[Ca^{2+}]_i$ ($nM \cdot min^{-1}$) following different modes of anoxia. C2C12 myotubes were loaded with fura-2 and $[Ca^{2+}]_i$ was followed with time. Anoxia was induced either by gassing the experimental solutions with N_2 or by the addition of sodium azide (10 mM) or sodium dithionite (20 mM). Values are calculated as the linear slope in the time range 2−20 min following anoxia. The numbers of independent experiments for oxygenated, N_2, dithionite, and azide were six, eight, five, and six, respectively. An asterisk (*) indicates significant difference from the oxygenated value.

(20 nCi/mL) for 2 h at 37 °C. The preincubation solution was aspirated, and the cells were washed five times with isosmotic KCl solution to remove excess extracellular [^{14}C]taurine. One milliliter of isosmotic solution was added to the dish after the final wash. At 2 min time intervals a 1 mL aliquot was transferred to a scintillation vial for estimation of ^{14}C activity (β-scintillation counting, Ultima Gold) and replaced by another 1 mL of experimental solution. The amount of [^{14}C]taurine remaining inside the cells was estimated at the end of the efflux experiment by treating the cells with 1 mL of 0.5 M NaOH for 1 h, washing the dishes two times with distilled water, and estimating the ^{14}C activity in the NaOH as well as in water washouts. The natural logarithm to the fraction of ^{14}C activity remaining in the cells at a given time (t) was plotted versus time, and the rate constant for the taurine efflux was estimated as the negative slope of the graph between time point t and its preceding time point.

Estimation of Amino Acid and Potassium Content in Drip Loss from Meat Samples. Danish landrace pigs (halothane negative and halothane positive) were used for quantitative and qualitative estimation of drip loss between 0 and 24 h, between 24 and 48 h, and between 48 and 72 h post-mortem. The meat samples (M. longissimus dorsi, 5 cm thick, 100 g) were removed from around the 10th rib, cut along the direction of the fibers, weighed, and immediately suspended in a net and sealed into an inflated plastic bag. After hanging at 4 °C for the 24 h time periods, the drip was collected and the meat slice reweighed. The drip loss was calculated as the percentage drip loss of the original weight. Samples for estimation of amino in meat 24 h post-mortem were weighed, freeze-dried for 24 h, reweighed, and suspended in borate buffer (pH 10.4). The content of taurine, alanine, glycine, and aspartic acid in the drip loss and meat samples was estimated by a standard OPA derivatization procedure followed by HPLC separation (Gilson 3222 pump; UV−vis-155). Briefly, samples were centrifuged (2000g, 4 °C, 10 min), the supernatant deproteinized by addition of sulfosalicylic acid (3% final concentration), placed on ice for 1 h, and centrifuged (2000g, 4 °C, 10 min). The final supernatant was filtered (Milex-GV, 0.45 μm) and 10 μL used for HPLC analysis. Separation was performed on a Nucleosil column (Macherey-Nagel, C18, 250/4, 5 μM), using a flow rate of 1 mL/min, and a eluent system in which the fraction of acetronitrile in a 12.5 mM phosphate buffer (pH 7.2) increased from 0 to 25% within 24 min and from 25 to 50% within the following 5 min. The amino acid concentration was estimated from the UV absorption (330 nm) of the samples and standards. The potassium content in the filtered supernatant was estimated by atomic flame photometry (Perkin-Elmer atomic absorption spectrophotometer, model 2380) as previously described in detail (*22*). Protein content was estimated using a standard Lowry procedure (*23*) with bovine serum albumin as standard.

Statistics. All values are given as means ± SEM. For all statistical evaluations significance was established at the 0.05 level. Statistical significance was evaluated with a Student t test for taurine efflux and drip loss data. Statistical comparisons of Ca^{2+} data were performed with one-way analysis of variance (ANOVA). When the ANOVA resulted in a significant F value ($P < 0.05$), the significant difference between means was located by the Fishers PLSD post hoc test. n is the number of experiments.

RESULTS AND DISCUSSION

Qualitative and Quantitative Characterization of Drip Loss. Drip loss has been related to the sensitivity to halothane (*24*), glycogen content in the muscle at the time of slaughter (*25*, *26*), and perimortal stress, which simultaneously accelerate the post-mortem acidification and increase in muscle temperature (*27*). To limit drip loss, various approaches have been used, for example, rapid chilling of the carcass, different forms of anesthetics before the animal is slaughtered, and genetic selection as well as inclusion of antioxidants in the food. However, the exact mechanism underlying drip loss is poorly understood.

The drip loss from M. longissimus dorsi of halothane-negative pigs was negligible within the first 24 h post-mortem (data not shown). However, drip loss represents 4.8 and 7.4% of the initial weight within 24−48 and 48−72 h post-mortem, respectively (Table 1). Thus, the rate of drip loss increases with time. Table 1 shows that the drip loss contains K^+ and amino acids, including taurine, as well as significant amounts of protein. Furthermore, the concentration, that is, the relative contribution, of the various compounds in the drip loss does not vary with time within the first 72 h post-mortem (Table 1). In contrast, drip loss from pigs carrying the halothane gene (heterozygous) showed, within 24−48 h post-mortem, a >2-fold higher loss compared to the halothane-negative pig (Table 1). This increased drip loss could reflect an increased loss of K^+ as well as taurine (Table 1).

Appearance of salts, proteins, amino acids, and water in the drip loss could reflect that a limited number of cells underwent autolysis and subsequently released their contents to the surroundings. Mammalian skeletal muscle cells contain a high concentration of K^+ (140 mM

Table 1. Weight Loss and K^+, Amino Acid, and Protein Concentrations in Drip from M. longissimus dorsi

time,[a] h	pig species	wt loss in %	K^+, mM	taurine, mM	alanine, mM	glycine, mM	aspartic acid, mM	protein, mg/mL	*n*
24−48	normal	4.8 ± 0.4	136 ± 3	13 ± 3	10 ± 3	7 ± 2	6 ± 2	129 ± 4	8
	halothane	11 ± 1	144 ± 3	23 ± 4	6 ± 1	9 ± 1	4.0 ± 0.8	114 ± 3	4
48−72	normal	7.4 ± 0.9	131 ± 3	18 ± 4	11 ± 3	8 ± 1	5.7 ± 0.3	123 ± 2	3

[a] Post-mortem.

Table 2. Effect of Channel Blocking Agents and Acidification on Anoxia-Induced Increase in $[Ca^{2+}]_i$ in C2C12 Myotubes

	treatment	target of agent	increase in $[Ca^{2+}]$, nM·min^{-1}	n	P^a
oxygenated	control		2.5 ± 0.7	6	<0.001
	low pH[b]		24 ± 1	4	<0.001
anoxia	anoxic control		32 ± 1	8	
N_2 buffered	low[c] extracellular Ca^{2+}		11 ± 3	5	<0.001
	verapamil, 10 μM	L-type Ca^{2+} channel	31 ± 2	4	NS
	tetrodotoxin, 1 μM	sarcolemma Na^+ channel	4.7 ± 0.9	6	<0.001
	saxitoxin, 100 nM	sarcolemma Na^+ channel	6 ± 1	5	<0.001
	ryanodine, 10 μM	SR Ca^{2+} release channel	31 ± 1	4	NS

[a] Values are compared to anoxic control value at pH 7.4. NS indicates nonsignificance at a 0.05 level. [b] The extracellular pH was reduced from standard 7.40 to 6.00. [c] The extracellular free Ca^{2+} was reduced from standard 1.2 mM to 0.2 mM.

≈ 90 mmol/kg of wet weight; *28*), protein, and amino acids. We have estimated the cellular taurine concentration in meat samples from a standard Danish pig 24 h post-mortem at 10.5 ± 0.5 mM (≈7.8 ± 0.4 mmol/kg of wet weight, $n = 3$), offering taurine a potential role as an organic osmolyte in muscle cells. From Table 1 it is seen that the K^+ and taurine concentrations in halothane-negative pigs are in the ranges of 131−136 and 13−18 mM, respectively. As the cellular concentrations and the concentration in drip are not different, this is taken to reflect a genuine increase in the permeability of the sarcolemmal membrane of the muscle toward cellular osmolytes.

$[Ca^{2+}]_i$ Increases during Anoxia. As an anoxic/ischemic condition in muscles as well as cellular acidification is inevitably associated with the slaughtering process, we have analyzed the consequence of anoxia and reduction of extracellular pH on $[Ca^{2+}]_i$ in the mouse myoblastic cell line C2C12. From Figure 1A it is seen that following anoxic exposure there is an initial 2 min lag phase whereafter $[Ca^{2+}]_i$ increases linearly with time. This observation supports previously reported results on mouse neocortical neurons in primary culture (*29*) and on whole muscle preparations (*30*). It is estimated that the increase in $[Ca^{2+}]_i$ in C2C12 cells is 2.5 nM·min^{-1} under oxygenated conditions and 32 nM·min^{-1} when anoxia is induced by gassing the experimental solutions with N_2 (Figure 1B and Table 2). Inducing chemical anoxia by addition of the potent reducing agent sodium dithionite or the respiratory chain inhibitor sodium azide leads to an increase in $[Ca^{2+}]_i$ of similar magnitude (20−30 nM·min^{-1}; Figure 1B). The increase in $[Ca^{2+}]_i$ following anoxia could be due to Ca^{2+} release from intracellular stores or Ca^{2+} influx from the extracellular compartment. To differentiate the possible sources of Ca^{2+}, we investigated the effect of addition of different ion channel blockers and reduction in the extracellular $[Ca^{2+}]$ in combination with anoxia (Table 2). Adding the sarcoplasmic reticulum Ca^{2+} release channel blocker ryanodine (10 μM) did not affect the anoxia-induced rise in $[Ca^{2+}]_i$. However, cells incubated with low extracellular Ca^{2+} concentration (0.2 mM) showed a marked depression in the rate of increase in $[Ca^{2+}]_i$, which strongly indicates that a substantial part of the increase in $[Ca^{2+}]_i$ is due to entry from the extracellular compartment. Verapamil (10 μM), which blocks the sarcolemma L-type Ca^{2+} channel, did not affect the anoxia-induced rise in $[Ca^{2+}]_i$, indicating that the anoxia-induced Ca^{2+} entry is not via the L-type Ca^{2+} channels. However, it has recently been shown that sarcolemma Na^+ channels can shift the ion selectivity to Ca^{2+} (*31*) and that excitation of skeletal muscle induces a considerable influx of Ca^{2+} via the Na^+ channels (*32*). We tested the hypothesis that the rise in $[Ca^{2+}]_i$ was due to entry of Ca^{2+} mediated by the Na^+ channels, by blocking the sodium channels with tetrodotoxine (TTX; 1 μM) or saxitoxine (100 nM). From Table 2 it is seen that TTX or saxitoxine almost completely blocked (93 and 88%, respectively) the anoxia-induced rise in $[Ca^{2+}]_i$. This indicates a crucial role of the Na^+ channel in the anoxia-induced rise in $[Ca^{2+}]_i$. Previously, it was shown that Na^+ channels are susceptible to ROS and that one of the main features was that cells, transiently exposed to H_2O_2, had significantly elevated $[Ca^{2+}]_i$ (*33*). Furthermore, it has been shown that thiol oxidation in the cells played a crucial role in the H_2O_2-induced Ca^{2+} dysregulation (*34*). The increase in $[Ca^{2+}]_i$ following exposure to oxidants seems to be a ubiquitous phenomenon in various cell types, including cardiomyocytes (*35*), vascular endothelial cells (*36*), smooth muscle cells (*37*), and hepatocytes (*38*). It is noted that the cellular Na^+ concentration increases during anoxia (see ref *17*), but whether this increase in cellular Na^+ stimulates Ca^{2+}/Na^+ exchange, that is, Ca^{2+} entry via a sarcolemma Na^+-Ca^{2+} exchanger, was not investigated in the present work.

Reducing the extracellular pH from 7.4 to 6.0 at oxygenated conditions also leads to a considerable increase in $[Ca^{2+}]_i$ (Table 2). Whether the effect of pH on $[Ca^{2+}]_i$ reflects reduced activity of the sarcoplasmatic reticulum Ca^{2+}-ATPase (*39*, *40*), reduced Ca^{2+} binding capacity of calcequestrin (see *41*), or a modification of sarcolemma Ca^{2+} transporting systems was not examined further.

C2C12 Cells and Primary Porcine Muscle Cells Possess Volume-Sensitive as well as LPC-Inducible Leak Pathways for Taurine. C2C12 cells have previously been shown to release taurine following hypotonic exposure (*42*). This is confirmed in Figure 2A and Table 3, where it is seen that dilution of the isotonic solution to 67% with water leads to a 120-fold increase in the rate constant for taurine efflux. It is noted that we used solutions containing high concentrations of K^+ in our taurine efflux experiments in order to prolong the volume-activated response in hyposmotic media (*43*). Panels A and B of Figure 2 demonstrate that taurine

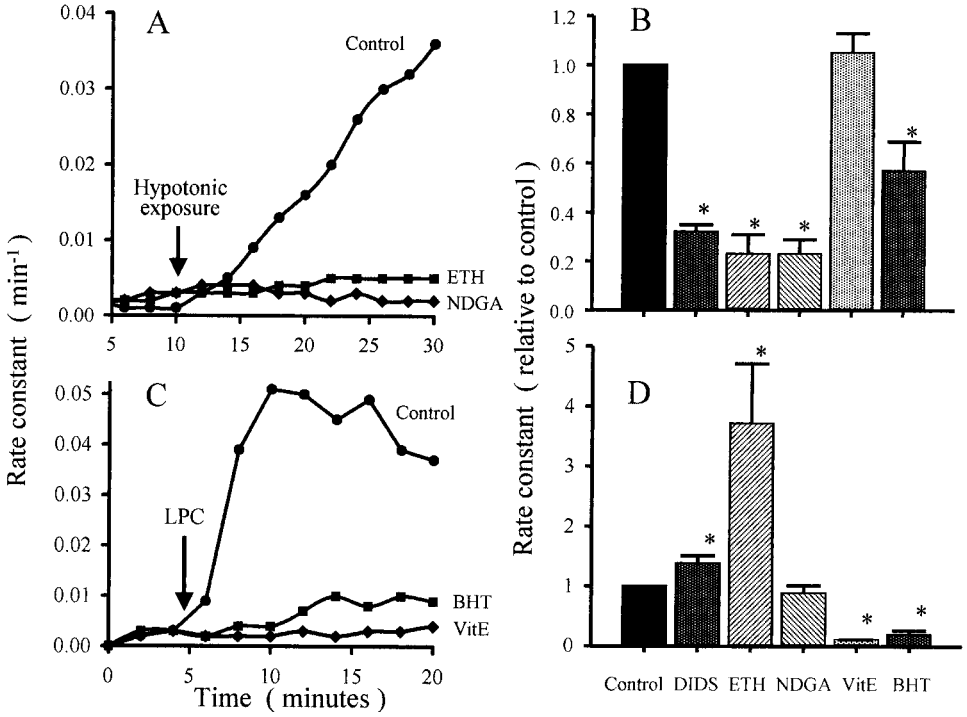

Figure 2. Regulation of swelling- and LPC-induced taurine release from C2C12 myotubes: (A, C) typical time courses for taurine release; (B, D) maximal rate constants for taurine release, after hypotonic cell swelling (B) or addition of LPC (D) in the absence (control) or presence of inhibitors and antioxidants, estimated and given relative to the control value. Cells were loaded with ^{14}C-labeled taurine for 2 h. The efflux was followed in isotonic KCl media with a shift, as indicated by the arrow, to either hypotonic KCl medium (210 mOsm, panels A and B) or isotonic KCl medium containing LPC (5 μM, panels C and D). The anion channel blocker DIDS (100 μM), the 5-LO inhibitors ETH 615-139 (10 μM) and NDGA (50 μM), and the antioxidants VitE (100 μg/mL) and BHT (10 mM), were added at the time of initiation of the release experiments. The absolute rate constant (min^{-1}) for the taurine efflux was calculated as described under Materials and Methods. The numbers of paired experiments for DIDS, ETH 615-139, NDGA, VitE, and BHT were four, three, three, five, and five (B) and four, five, three, four, and four (D), respectively. An asterisk (*) indicates significant difference from control value.

Table 3. Effect of Ca^{2+} Mobilization, Cell Swelling, and Addition of LPC on $[Ca^{2+}]_i$ and the Rate Constant for Taurine Release in C2C12 Myotubes

	increase in free cellular $[Ca^{2+}]$,[a] nM·min^{-1}	rate constant for taurine release,[b] min^{-1}
isotonic, 300 mOsm		
control	2.5 ± 0.7 (n = 6)	0.0023 ± 0.0002 (n = 52)
5 μM LPC	15 ± 2 (n = 5)*	0.032 ± 0.005 (n = 15)*
10 μM LPC	19 ± 1 (n = 6)*	0.066 ± 0.010 (n = 10)*
10 μM ATP	495 ± 64 (n = 5)[c]*	0.004 ± 0.001 (n = 3)
hypotonic, 210 mOsm		
control	2.3 ± 0.4 (n = 6)	0.028 ± 0.002 (n = 17)*
10 μM ATP		0.061 ± 0.018 (n = 5)#

[a] Ca^{2+} values are calculated as the linear slope in the time range from 2 to 20 min following hypotonic exposure/addition of LPC. *, significantly different from isotonic values. [b] Maximal rate constant. #, significantly different from hypotonic value. [c] Peak value following addition of ATP.

release following hypotonic exposure is reduced in the presence of the 5-LO inhibitors nordihydroguaiaretic acid (NDGA; antioxidant-type of inhibitor; *12*) and ETH 615-139 (direct inhibitor; *44*). Thus, 5-LO activity is required for the swelling-induced activation of taurine release in C2C12 cells. On the other hand, swelling-induced taurine release from C2C12 cells is not affected in the presence of the lipophilic antioxidant VitE and only marginally affected by the water soluble antioxidant butylated hydroxytoluene (BHT).

An LPC-sensitive taurine efflux pathway, separate from the volume-sensitive taurine efflux pathway, has recently been demonstrated in HeLa cells (*13*), Ehrlich cells (*10*, *14*), and mouse fibroblasts (*11*, *13*). Taurine is also released from C2C12 cells under isotonic conditions following the addition of 5 μM LPC (Figure 2C). Furthermore, the effect of LPC is concentration dependent (Table 3), impaired in the presence of the antioxidants VitE and BHT (Figure 2C,D), and unaffected by the addition of NDGA (Figure 2D). From Figure 2D it is seen that the effect of LPC is potentiated in the presence of ETH 615-139. The LPC-induced taurine efflux is also potentiated in the presence of oxidants; that is, the maximal rate constant for LPC (5 μM) induced taurine efflux was increased 2.8 ± 0.2-fold in the presence of 2 mM H_2O_2 (n = 5; P = 0.04). Thus, it appears that LPC-induced taurine release in C2C12 cells involves generation of ROS and is independent of 5-LO activity. Whether the potentiating effect of the 5-LO inhibitor ETH 615-139 on the LPC-induced taurine release reflects an effect of ETH 615-139 on the ROS homeostasis was not investigated. The swelling-induced taurine release and the LPC-induced taurine release in HeLa cells, for example, are distinguished by their sensitivity to the anion channel blocker diisothiocyanatostilbene-2,2′-disulfonic acid (DIDS) (*13*). This is also the case in C2C12 cells, where DIDS (100 μM) reduces the volume-sensitive taurine efflux by 70%, whereas it potentiates the LPC-induced taurine release (Figure 2B,D). Thus, C2C12 cells have at least two taurine efflux pathways, that is, a volume-sensitive, DIDS-sensitive pathway, which requires 5-LO activity for activation, and an LPC-inducible, DIDS-insensitive pathway, which involves production of ROS for activation.

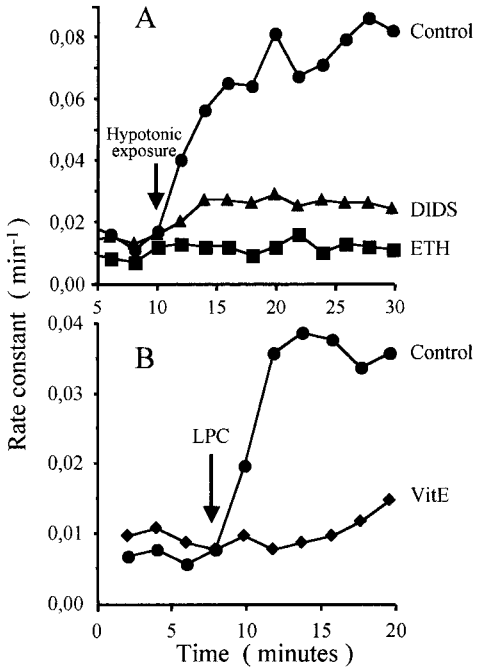

Figure 3. Time courses for swelling- and LPC-induced taurine release from porcine primary myotubes. Cells were loaded with ^{14}C-labeled taurine for 12 h. The efflux was followed in isotonic KCl medium with a shift, as indicated by the arrow, to either hypotonic KCl medium (210 mOsm, panel A) or isotonic KCl medium containing LPC (5 μM, panel B). The anion channel blocker DIDS (100 μM), the 5-LO inhibitor ETH 615-139 (10 μM), and the antioxidant VitE (100 μg/mL) were added at the time of initiation of the release experiments. The maximal rate constant for the taurine efflux, calculated as described under Materials and Methods, was estimated at 0.090 ± 0.015 min^{-1} ($n = 3$) following hypotonic cell swelling and at 0.038 ± 0.002 min^{-1} following addition of LPC ($n = 3$).

From Figure 3 it is seen that primary porcine muscle cells, just like the C2C12 cells, release taurine following hypotonic exposure and addition of LPC. The hypotonic taurine efflux is sensitive to DIDS and ETH 615-139 (Figure 3A), whereas the LPC-induced taurine efflux is abolished in the presence of the antioxidant VitE (Figure 3B). Thus, the presence of taurine and other amino acids reported in the drip from Danish landrace pigs (Table 1) could reflect loss from the muscle via the volume-sensitive and/or the LPC-inducible leak pathways. The mechanisms responsible for the K^+ appearance in the drip were not investigated further.

Ca^{2+} Modulates the Swelling-Induced Taurine Release. A pathological elevation of $[Ca^{2+}]_i$ following anoxia has been shown to activate several Ca^{2+}-dependent cytotoxic mechanisms, that is, disruption of the cytoskeletal network as well as activation of catabolic enzymes (proteases, e.g., calpains), endonucleases, and phospholipases. Phospholipases catalyze the hydrolysis of membrane phospholipids, and a number of studies have indicated an accelerated phospholipid turnover occurs during anoxia (*45*−*47*). Hence, a sustained increase in $[Ca^{2+}]_i$ can result in enhanced breakdown of membrane phospholipids and, in turn, loss of cell integrity. The $[Ca^{2+}]_i$ during normal conditions is ~100 nM; that is, the $[Ca^{2+}]_i$ is 4 orders of magnitude lower than the concentration in the extracellular compartment and the sarcoplasmatic reticulum. The low cellular concentration is maintained by various active transport processes that remove Ca^{2+} from the cytosol, thereby counteracting the influx of Ca^{2+} from both internal and external stores. It has previously been shown that the Ca^{2+} mobilizing agonist thrombin and hypotonicity synergistically activate taurine efflux in proliferating C2C12 cell cultures (*42*). On the other hand, the effect of the thrombin-induced increase in $[Ca^{2+}]_i$ on taurine efflux vanishes as C2C12 cells differentiate into myotubes (*42*). From Table 3 it is seen that swelling-induced taurine release is not accompanied by any detectable increase in $[Ca^{2+}]_i$, whereas LPC induces taurine release as well as an increase in $[Ca^{2+}]_i$. An increase in $[Ca^{2+}]_i$ per se, induced by either addition of ATP (Table 3) or addition of thrombin (*42*), does not elicit taurine release in C2C12 myotubes suspended in isotonic solution. On the other hand, the maximal rate constant for taurine release following osmotic cell swelling is significantly increased when 10 μM ATP is added at the time of hypotonic exposure (Table 3). Thus, although an increase in $[Ca^{2+}]_i$ seems not to be a prerequisite for activation of the volume-sensitive taurine-releasing systems in C2C12 myotubes, it potentiates the rate of the swelling-induced taurine release, that is, loss of osmolytes and cell water.

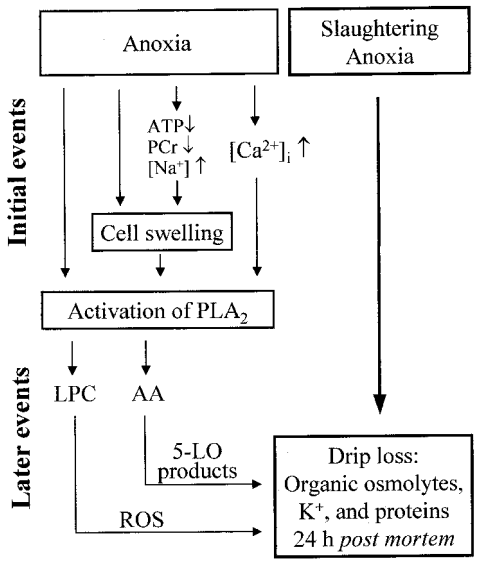

Figure 4. Hypothetical model for events in drip formation. Abbreviations: PCr, creatine phosphate; PLA_2, phospholipase A_2; LPC, lysophosphatidyl choline; AA, arachidonic acid; 5-LO, 5-lipooxygenase; ROS, reactive oxygen species. See text for details.

Model for Initial Events Underlying the Formation of Drip Loss. Figure 4 is a putative model illustrating events involved in the formation of drip loss from porcine muscle. The data in Table 1 indicated that the drip loss, obtained 24 h post-mortem, contained K^+, amino acids, and protein. It is emphasized that even though the osmolytes first become detectable in the drip ~24 h post-mortem, we assume that the processes leading to the formation of drip loss are initiated already during the transportation and stalling of livestock, stunning procedure, and handling of the carcasses.

From the model in Figure 4 it is indicated that PLA_2 activity leads to formation of arachidonic acid (AA) and lysophospholipids, that is, LPC, and thereby plays a key role in the swelling-induced as well as in the LPC-mediated release of osmolytes. The true identity of the activation mechanisms for the PLA_2 involved in the formation of drip loss are at present unknown. On the basis of their molecular size, Ca^{2+}-sensitivity, and substrate specificity, the PLA_2 have been divided into

four types: (i) the secretory, Ca^{2+}-dependent PLA_2 ($sPLA_2$); (ii) the cytosolic, Ca^{2+}-dependent PLA_2 ($cPLA_2$); (iii) the intracellular, Ca^{2+}-independent PLA_2 ($iPLA_2$); and (iv) phospholipases that prefer phospholipids with short chains in the *sn*-2 position (see ref *48*). Mammalian cells generally contain more than one type of PLA_2. As anoxia is accompanied by cell swelling, it is assumed that one of the initial events in the formation of drip loss (see Figure 4) is the activation of volume-sensitive osmolyte-releasing systems. In this context it should be noted that it appears to be a $cPLA_2$ that is involved in the volume regulatory processes in, for example, Ehrlich cells (*49*). As $cPLA_2$ and $sPLA_2$ are both Ca^{2+}-dependent, they are activated following an increase in $[Ca^{2+}]_i$ or exposure to the high Ca^{2+} concentration in the extracellular compartment. Free radicals also activate PLA_2 due to either peroxidation of lipids, reduction in membrane fluidity, or oxidation of protein side chains or SH formation (see ref *17*). It is assumed that in the propagation phase of drip loss formation, $sPLA_2$ and/or $iPLA_2$ becomes involved in the formation of LPC and that the activity of the enzymes is amplified by a positive feedback mechanism involving the ROS.

Increased ROS production during anoxia/ischemia could be caused by either an altered mitochondrial function, cellular acidification, increased xanthine oxidase activity, accumulation of monoamine, oxidation of accumulated AA via the cyclooxygenase and/or the 5-LO pathways, or activation of nitrogen oxide synthases (see ref *17*). An increase in ROS will inevitably affect peroxidation of cellular membrane lipids and proteins and thereby modulate the cell integrity, that is, permeability of the plasma membrane toward osmolytes.

Events That Affect Drip Loss. To limit loss of osmolytes, one should consider the limitation of (i) cell swelling and the subsequent activation of PLA_2/5-LO and volume-sensitive osmolyte leak pathways, (ii) the LPC-induced pathway involving ROS, and (iii) the increase in $[Ca^{2+}]_i$. The initial cell swelling is most probably due to the reduction in the availability of energy-rich phosphate compounds (ATP, PCr) and a subsequent net uptake of Na^+ (Cl^-) and water. Reducing the ambient humidity and temperature would most probably limit the initial cell swelling and the subsequent enzyme activity, as well as the activity of volume-sensitive osmolyte transporters. In this context it is noted that lowering the temperature from 37 to ~20 °C (room temperature) delays the onset and reduces the magnitude of ion currents via volume-sensitive K^+ and Cl^- channels in, for example, Ehrlich cells (*50*). The presence of unspecific antioxidants and chilling would reduce the effects mediated by the ROS. In this context, it is noted that meat from pigs fed vitamin E has a profoundly reduced drip loss (*51*). Anoxia-induced increase in $[Ca^{2+}]_i$ is unavoidable in muscle/meat considered for human consumption. However, as an increase in $[Ca^{2+}]_i$ seems to potentiate the initiation (amplification of swelling-induced osmolyte release) and the propagation (activation of proteases and phospholipases) of drip formation, one should focus on limiting (i) stress-induced Ca^{2+} mobilization and (ii) the Ca^{2+}-amplified/induced events in order to limit drip loss.

Conclusion. Using (i) the qualitative characterization of drip and (ii) a C2C12 myotube muscle plus primary porcine muscle cell systems to simulate the physiological events taking place during slaughter, we present a tentative model for events preceding the formation of drip. Anoxia following slaughter is assumed to induce a rise in $[Ca^{2+}]_i$, activation of PLA_2, and subsequent formation of AA and LPC. AA and LPC lead to net loss of cellular osmolytes via 5-LO products and ROS, respectively.

LITERATURE CITED

(1) Offer, G.; Knight, P. The structural basis of water-holding in meat Part 2: Drip losses. In *Developments in Meat Science—4*; Lawrie, R., Ed.; Elsevier Applied Science: London, U.K., 1988; Chapter 4, pp 172−243.

(2) Tornberg, E.; Andersson, A.; Göransson, Å.; Set, G. von. Water and Fat Distribution in Pork in Relation to Sensory Properties. In *Pork Quality: Genetic and Metabolic Factors*; Puolanne, Ed., Demeyer, D. I., with Ruusunen, M., Ellis, S., Eds.; CABI: Wallingford, U.K., 1993, pp 239−258.

(3) Kuntz, I. D.; Kaufmann, W. Hydration of proteins and polypeptides. *Adv. Protein Chem.* **1974**, *28*, 239−345.

(4) Oeckel, M. J.; Warnants, van N.; Boucque, C. V. Comparison of different methods for measuring water holding capacity and juiciness of pork versus on-line screening methods. *Meat Sci.* **1999**, *51*, 313−320.

(5) Maribo, H.; Olsen, E. V.; Barton-Gade, P.; Møller, A. J.; Karlsson, A. Effect of Early Post-Mortem Cooling on Temperature, pH Fall and Meat Quality in Pigs. *Meat Sci.* **1998**, *59*, 115−129.

(6) Taylor, A. A.; Dant, S. J. Influence of carcass cooling rate on drip loss in pigmeat. *J. Food Technol.* **1971**, *6*, 131−139.

(7) Zarate, J. R.; Zaritzky, N. E. Production of weep in packaged refrigerated beef. *J. Food Sci.* **1985**, *50*, 155−159.

(8) Lang, F.; Busch, G. L.; Ritter, M.; Völkl, H.; Waldegger, S.; Gulbins, E.; Häussinger, D. Functional significance of cell volume regulatory mechanisms. *Physiol. Rev.* **1998**, *78*, 247−306.

(9) Hoffmann, E. K.; Mills, J. W. Membrane events involved in volume regulation. *Curr. Top. Membr.* **1999**, *48*, 123−196.

(10) Lambert, I. H. Regulation of the taurine content in Ehrlich ascites tumour cells. In *Taurine 3: Cellular and Regulatory Mechanisms*; Schaffer, S., Lombardini, J. B., Huxtable, R. J., Eds.; Plenum Publishing: New York, 1998; pp 269−276.

(11) Lambert, I. H.; Sepúlveda F. V. Swelling-induced taurine efflux from HeLa cells. In *Taurine 4: Taurine and Excitable Tissues*; Della Corte, L., Huxtable, R. J., Sgaragli, G. P., Tipton, K. F., Eds.; Kluwer Academic/Plenum Publishing: New York, 2000; pp 487−496.

(12) Musser, J. H.; Kreft, A. F. 5-Lipoxygenase: Properties, Pharmacology, and the Quinolinyl(bridged)aryl Class of Inhibitors. *J. Med. Chem.* **1992**, *35*, 2501−2524.

(13) Lambert, I. H.; Falktoft, B. Lysophosphatidylcholine induces taurine release from HeLa cells. *J. Membr. Biol.* **2000**, *176*, 175−185.

(14) Lambert, I. H.; Falktoft, B. Lysophosphatidylcholine-induced taurine release in HeLa cells involves kinase activity. *Comp. Biochem. Physiol.* **2001**, *130*, 577−584.

(15) Shaikh, N. A.; Downar, E. Time course of changes in porcine myocardial phospholipid levels during ischemia. A reassessment of the lysolipid hypothesis. *Circ. Res.* **1981**, *49*, 316−325.

(16) Liu, S. Y.; Lu, X.; Choy, S.; Dembinski, T. C.; Hatch, G. M.; Mymin, D.; Shen, X.; Angel, A.; Choy, P. C.; Man, R. Y. K. Alteration of lysophosphatidylcholine content in low-density lipoprotein after oxidative modification: Relationship to endothelium dependent relaxation. *Cardiovasc. Res.* **1994**, *28*, 1476−1481.

(17) Lipton, P. Ischemic cell death in brain neurons. *Physiol. Rev.* **1999**, *79*, 1432−1568.

(18) Yaffe, D.; Saxel, O. Serial passaging and differentiation of myogenic cells isolated from dystrophic mouse muscle. *Nature* **1977**, *270*, 725−727.

(19) Bischoff, R. Enzymatic liberation of myogenic cells from adult rat muscle. *Anat. Rec.* **1974**, *180* (4), 645−661.
(20) Grynkiewicz, G.; Poenie, M.; Tsien, R. Y. A new generation of Ca^{2+} indicators with greatly improved fluorescence properties. *J. Biol. Chem.* **1985**, *260*, 3440−3450.
(21) Hall, J. A.; Kirk, J. A.; Potts, J. R.; Rae, C.; Kirk, K. Anion channel blockers inhibit swelling-activated anion, cation, and nonelectrolyte transport in HeLa cells. *Am. J. Physiol.* **1996**, *271*, C579−C588.
(22) Hoffmann, E. K.; Simonsen, L. O.; Sjøholm, C. Membrane potential, chloride exchange, and chloride conductance in Ehrlich mouse ascites tumour cells. *J. Physiol.* **1979**, *296*, 61−84.
(23) Lowry, O. H.; Rosenbrough, N. J.; Farr, A. L.; Randall, R. J. Protein measurement with the Folin phenol reagent. *J. Biol. Chem.* **1951**, *193*, 255−275.
(24) Cheah, K. S.; Cheah, A. M.; Krausgril, D. I. Variations in meat quality in live halothane heterozygotes identified by biopsy samples of M. longissimus dorsi. *Meat Sci.* **1995**, *39* (2), 293−300.
(25) Bendall, J. R. *Post mortem* changes in muscle. In *Structure and Function of Muscle*; Bourne, G. H., Ed.; Academic Press: New York, 1973; pp 243−309.
(26) Warris, P. D.; Bevis, E. A.; Ekins, P. J. The relationships between glycogen stores and muscle ultimate pH in commercially slaughtered pigs. *Br. Vet. J.* **1989**, *145*, 378−383.
(27) Karlsson, A. H.; Henckel, P.; Andersson, M. Early estimation of ultimate pig meat quality. Presented at the Annual Meeting of the European Association of Animal Production, Vienna, Austria, 1997; p 181.
(28) Sejersted, O. M.; Sjøgaard, G. Dynamics and consequences of potassium shifts in skeletal muscle and heart during exercise. *Physiol. Rev.* **2000**, *80*, 1411−1481.
(29) Jørgensen, N. K.; Petersen, S. F.; Damgaard, I.; Schousboe, A.; Hoffmann, E. K. Increases in $[Ca^{2+}]_i$ and changes in intracellular pH during chemical anoxia in mouse neocortical neurons in primary culture. *J. Neurosci. Res.* **1999**, *56*, 358−370.
(30) McCall, K. E.; Duncan, C. J. Independent pathways causing cellular damage in mouse soleus muscle under hypoxia. *Comp. Biochem. Physiol.* **1989**, *94*, 799−804.
(31) Santana, L. F.; Gomez, A. M.; Lederer, W. J. Ca^{2+} flux through promiscuous cardiac Na^+ channels: slip-mode conductance. *Science* **1998**, *279*, 1027−1033.
(32) Gissel, H.; Clausen, T. Excitation-induced Ca^{2+} uptake in rat skeletal muscle. *Am. J. Physiol.* **1999**, *276*, R331−R339.
(33) Joseph, J. A.; Strain, J. G.; Jimenez, N. D.; Fisher, D. Oxidant injury in PC12 cells—a possible model of calcium "dysregulation" in aging: I. Selectivity of protection against oxidative stress. *J. Neurochem.* **1997**, *69*, 1252−1258.
(34) Wang, H.; Joseph, J. A. Mechanisms of hydrogen peroxide-induced calcium dysregulation in PC12 cells-(1). *Free Radical Biol. Med.* **2000**, *28*, 1222−1231.
(35) Kaminishi, T.; Matsuoka, T.; Yanagishita, T.; Kako, K. J. Increase vs decrease of calcium uptake by isolated heart cells induced by H_2O_2 vs HOCl. *Am. J. Physiol.* **1989**, *256*, C598−C607.
(36) Hinshaw, D. B.; Burger, J. M.; Armstrong, B. C.; Hyslop, P. A. Mechanism of endothelial cell shape change in oxidant injury. *J. Surg. Res.* **1989**, *46*, 339−349.
(37) Roveri, A.; Coassin, M.; Maiorino, M.; Zamburlini, A.; van Amsterdam, F. T.; Ratti, E.; Ursini, F. R. Effect of hydrogen peroxide on calcium homeostasis in smooth muscle cells. *Arch. Biochem. Biophys.* **1992**, *297*, 265−270.
(38) Albano, E.; Bellomo, G.; Parola, M.; Carini, R.; Dianzani, M. U. Stimulation of lipid peroxidation increases the intracellular calcium content of isolated hepatocytes. *Biochim. Biophys. Acta* **1991**, *1091* (3), 310−316.
(39) Inesi, G.; Hill, T. L. Calcium and proton dependence of sarcoplasmic reticulum ATPase. *Biophys. J.* **1983**, *44*, 271−280.
(40) Lamb, G. D.; Jukanar, P. R.; Stephenson, D. G. Effects of myoplasmic pH on excitation-contraction coupling in skeletal muscle fibres of the toad. *J. Physiol.* **1992**, *448*, 211−224.
(41) Donoso, P.; Beltran, M.; Hidalgo, C. Luminal pH regulated calcium release kinetics in sarcoplasmic reticulum vesicles. *Biochemistry* **1996**, *35*, 13419−13425.
(42) Manolopoulos, V. G.; Droogmans, G.; Nilius, B. Hypotonicity and thrombin activate taurine efflux in BC_3H1 and C_2C_{12} myoblasts that is down regulated during diffentiation. *Biochem. Biophys. Res. Commun.* **1991**, *232*, 74−79.
(43) Kirk, J.; Kirk, K. Volume-regulatory taurine release from a human lung cancer cell line. Evidence for amino acid transport via a volume-activated chloride channel. *FEBS* **1993**, *336*, 153−158.
(44) Kirstein, D.; Thomsen, M. K.; Ahnfelt-Rønne, I. Inhibition of leukotriene biosynthesis and polymorphonuclear leukocyte functions by orally active quinolylmethoxyphenylamines. *Pharmacol. Toxicol.* **1991**, *68*, 125−130.
(45) Choi, K. H.; Edelstein, C. L.; Gengaro, P.; Schrier, R. W.; Nemenoff, R. A. Hypoxia induces changes in phospholipase A_2 in rat proximal tubules: evidence for multiple forms. *Am. J. Physiol.* **1995**, *269*, F846−F853.
(46) Portilla, D.; Mandel L. J.; Bar-Sagi, D.; Millington, D. S. Anoxia induces phospholipase A_2 activation in rabbit renal proximal tubules. *Am. J. Physiol.* **1992**, *262*, F354−F360.
(47) Farber, J. L.; Young, E. E. Accelerated phospholipid degradation in anoxic rat hepatocytes. *Arch. Biochem. Biophys.* **1981**, *211*, 312−320.
(48) Balsinde, J.; Balboa, M. A.; Insel, P. A.; Dennis, E. A. Regulation and inhibition of phospholipase A_2. *Annu. Rev. Pharmacol. Toxicol.* **1999**, *39*, 175−189.
(49) Thoroed, S. M.; Lauritzen, L.; Lambert, I. H.; Hansen, H. H.; Hoffmann, E. K. Cell swelling activates phospholipase A_2 in Ehrlich ascites tumour cells. *J. Membr. Biol.* **1997**, *160*, 47−58.
(50) Riquelme, G.; Sepulveda, F. V.; Jørgensen, F.; Pedersen S.; Hoffmann, E. K. Swelling-activated potassium currents of Ehrlich ascites tumour cells. *Biochim. Biophys. Acta* **1998**, *1371*, 101−106.
(51) Monahan, F. J.; Gray, J. I.; Asghar, A.; Haug, A.; Strasburg, G. M.; Buckley, D. J.; Morrissey, P. A. Influence of diet on lipid oxidation and membrane structure in porcine muscle microsomes. *J. Agric. Food Chem.* **1994**, *42*, 59−63.

Received for review January 29, 2001. Revised manuscript received June 26, 2001. Accepted July 5, 2001. This work was supported by the Danish Bacon and Meat Council and the Danish Natural Sciences Research Council.

JF010121Y